Materials Research Proceedings 34 (2023) 43-52 https://doi.org/10.21741/9781644902691-6

Microstructural Analysis of Wound Composites with Considerations on the Fiber Winding Force

KRYSIAK Piotr

Military Institute of Engineer Technology, Obornicka 136 Street, 50-961 Wrocław, Poland

krysiak@witi.wroc.pl

Keywords: Resin, Carbon Fiber, Glass Fiber, Composite, Microstructural Analysis

Abstract. The paper concerns issues related to the fabrication and microstructural analysis of carbon and glass fiber-reinforced epoxy composites. For the purposes of the tests, ring samples of carbon fiber and glass fiber were fabricated, each sample being made of the same amount of material. The rings were produced by circumferentially wrapping fibers onto a rigid core. During winding, the fiber tension was changed for each sample to investigate whether the amount and distribution of fibers in the composite depending on the force applied. The applied tension forces ranged from 18 to 138 N. In the next stage of tests, small fragments were cut out of the rings, cutting perpendicularly to the arrangement of fiber bundles. The cut elements were then embedded in epoxy resin. The microsections prepared in this were ground using a grinding disc with a gradation of 80 to 4000 and then polished, washed and dried. After these treatments, microscopic photos of the tested surfaces were taken. Observations were made using a NEOPHOT 32 microscope with an integrated camera and a KEYENCE VHX microscope. The volume fraction of voids and discontinuities in the matrix, as well as the volume fraction of fibers, were determined by measuring the percentage of the surface areas occupied by the appropriate components of the composite. On each cross-section of individual samples, photographs were taken in three planes parallel to the composite layers and three planes perpendicular to the fibers – in the matrix system. The image analysis method was used for verification, in which it is assumed that the assessment of fiber distribution in a two-dimensional section is representative of its volumetric distribution. This method is mainly used to analyze the distribution of fibers with a constant cross-section. The most important conclusions from the conducted analyses allow the authors to state that in both composites the fibers in the matrix are highly packed and that there was no significant and noticeable effect of fiber tension during winding on the "packing" density of fibers in the composites.

Introduction

A significant group of products made of reinforced plastics are pipes and high-pressure tanks, made by winding. They effectively replace products made of traditional construction materials in many technical fields. An essential factor for the increase in the use of these materials in wound products is the knowledge of the impact of manufacturing technology on the performance properties, as these materials are characterized by high anisotropy of mechanical properties. This anisotropy is created in the manufacturing process and can be freely adjusted depending on the intended use of the structure and the type of loads. In composite fibrous structures, the main load is carried by the fibers, while the binder (resin) binds the composite and ensures the fixation/solidification of the given shape of the product [1, 2].

Unidirectionally reinforced composites are the basic composites and, at the same time, the easiest ones to describe. As a result of the reinforcement, a macroscopically isotropic composite is formed in a plane perpendicular to the direction of the reinforcement, i.e. a composite with transversely isotropic symmetry. Since these groups of composites have a wide practical

application, the problem of predicting the elastic properties of a unidirectionally reinforced composite based on the properties of its components becomes vital. There are many models describing these kinds of materials. Typically, the authors of these models adopted the linear-elastic properties of the fibers and matrix, and the hypothesis of flat cross-sections is commonly accepted in the strength of materials [4, 6, 7, 8].

Material Preparation for the Tests

In order to determine the actual mechanical properties of the materials (composites) used for the tests, samples with ring geometry were produced by the winding method, each sample being made of the same amount of fibers. During the winding process, the roving tension was changed for each sample.

In the presented studies, to produce test samples, "continuous" fibers in the form of roving, wound on a suitable core, were used. The exact properties of glass fibers are given in Table 1 [9], and carbon fibers in Table 2 [10].

Table 1. *Physical and mechanical properties of ER 3005 glass fiber (Krosglass)*

Property	**Value**
Longitudinal modulus of elasticity [GPa]	73
Tensile strength [MPa]	3400
Poisson's ratio [–]	0.21
Elongation at break [%]	3.5
Density [g/cm3]	2.55
Linear density [tex]	1200±7%
Monofilament diameter [μm]	10÷15

Table 2. *Properties of UTS 5631 12K carbon fiber (TohoTenax)*

Property	**Value**
Longitudinal modulus of elasticity [GPa]	240
Tensile strength [MPa]	4800
Poisson's ratio [–]	0.285
Elongation at break [%]	$-0.1 \cdot 10^{-6}$
Density [g/cm3]	1.8
Linear density [tex]	1.79
Monofilament diameter [μm]	800
Number of monofilaments	12000
Monofilament diameter [μm]	6.9
Rowing width [mm]	2.99

Epolam 5015 epoxy resin and AXSON Epolam 2016 hardener were used in the composite matrix. The properties of the cured resin are given in Table 3 [11].

Using this method, three rings were made of carbon fiber (epoxy/carbon) and glass fiber (epoxy-glass) with the tensile strength of the fibers of 18 N; 78N; 138 N, (Fig. 1).

Materials Research Proceedings 34 (2023) 43-52 https://doi.org/10.21741/9781644902691-6

Table 3. *Properties of Epolam 5015 (Axson) resin*

Property	**Value**
Flexural modulus [GPa]	2.9
Tensile strength [MPa]	73
Elongation at break [%]	7
Poisson ratio [–]	0.35
Hardness [Shore D15]	84
Mixing ratio [by weight]	32
Density at 25°C [g/cm3]	1.12÷1.16
Pot life (on 500 g) at 25°C [min.]	360÷450
Glass transition temperature [°C]	81
Brookfield viscosity at 25°C [mPa·s]	400÷500

a) b)

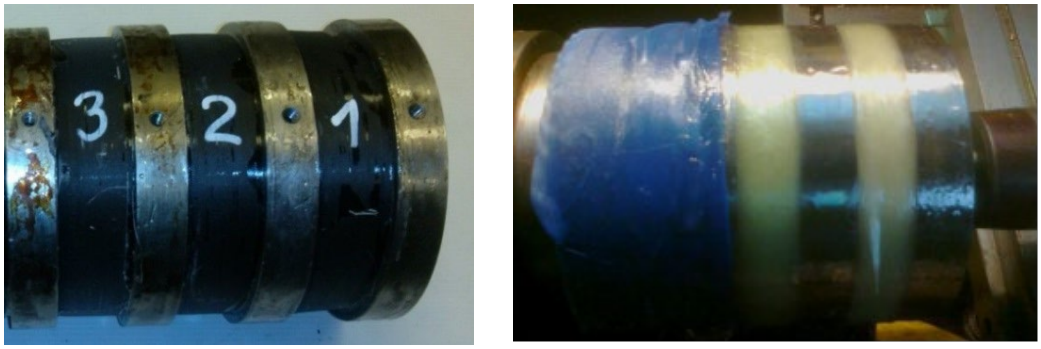

Fig.1. *Samples during the winding process; a –carbon samples, b – glass samples*

Fig.2. *The samples prepared for mechanical processing*

In the next stage, small fragments were cut out of the rings; it was done by cutting perpendicularly to the arrangement of fiber bundles. The cut elements were then embedded in epoxy resin. The microsections prepared in this way were ground on discs with a gradation of 80 to 4000 and then polished, washed and dried. Fig. 2 shows the preparation of sample sections for grinding.

Afterwards, the microscopic structure of the produced composites was examined to determine the volume fraction of fibers in the matrix. This is a key parameter affecting the material constants because the strength of the composite is mainly determined by the fibers it contains.

Materials Research Proceedings 34 (2023) 43-52 https://doi.org/10.21741/9781644902691-6

The observations were made with a NEOPHOT 32 microscope with an integrated camera and a KEYENCE VHX microscope.

The obtained microscopic images of the structures were analyzed in particular in terms of two factors:

– the number and distribution of defects in the form of discontinuities in the matrix filling;
– surface distribution and volume content of fibers in the composite.

Determination of the volume of fibers, matrix and voids in the analyzed structures was performed by image analysis.

The basic assumption of this method is that the assessment of fiber distribution in a two-dimensional section is representative of the volumetric distribution. This method is mainly used to analyze the distribution of fibers characterized by constant cross-section, as for the structures analyzed in this work. The method is described in more detail in [3].

The purpose of the method is to distinguish the color border between the fibers and the matrix, so in the first stage, the image should be reduced to a grey scale. The threshold value of individual colors can be determined based on histogram analysis (fig. 3).

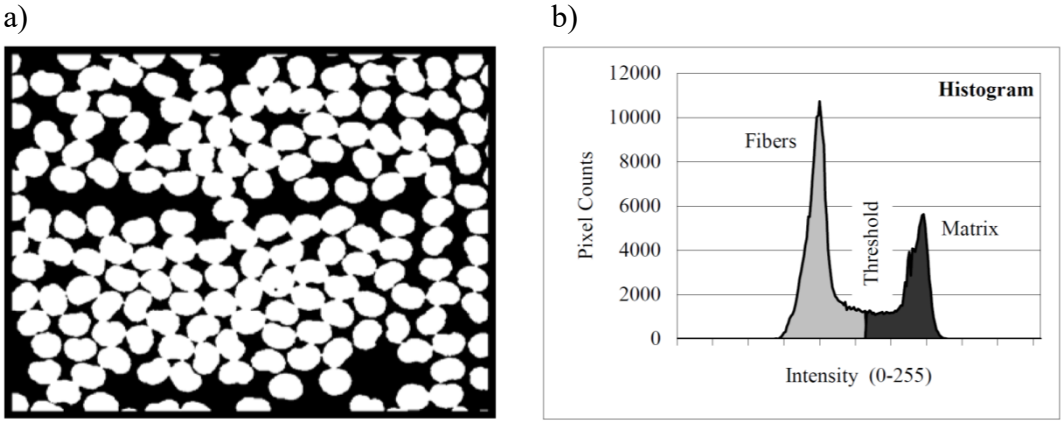

Fig.3. *Elements of image analysis; a – image of the cross-section of the sample in greyscale, b – typical histogram of fiber and resin distribution in greyscale*

The histogram shows the proportion of white and black colors (fiber and resin respectively, or vice versa). The computer then counts the number of pixels for the corresponding colors, and the ratio of these values to the total number of pixels determines the percentage of each component in the composite.

Microscopic Analysis of the Composites

The prepared surfaces of the samples were analyzed under a microscope at the following magnifications:

– ×50, to determine the distribution of roving strips and the volume fraction of voids in the composite;
– ×200, to illustrate the size of the structure discontinuity;
– ×500 or 1000, to determine the distribution of fibers in the matrix and their percentage share in the composite.

The volume fraction of voids and discontinuities in the matrix as well as the volume fraction of fibers were determined by measuring the percentage content of the surface areas occupied by the appropriate components of the composite. On each cross-section of individual samples, photographs were taken in three planes parallel to the layers and in three perpendicular ones – in the matrix system (Fig. 5).

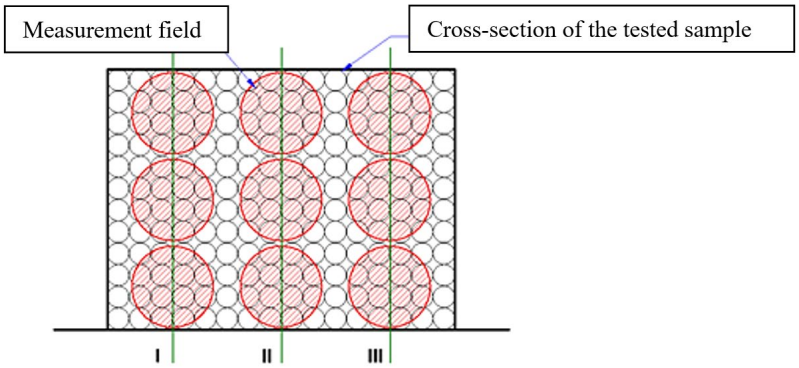

Fig.4. *Distribution of the tested fields on the cross-section of the samples*

Analysis of the microstructure of the epoxy/carbon fiber-reinforced composite. In the first stage, the share of voids and structure discontinuities was analyzed at ×50 magnification (Fig. 5). After determining the content of voids, the content of the remaining components of the composite, i.e. fibers and resin, was analyzed at ×200 and ×500 magnification (Fig. 6 and 7, Table 4). In addition, photos of the topography of the sample surface were taken (example photograph: Fig. 8).

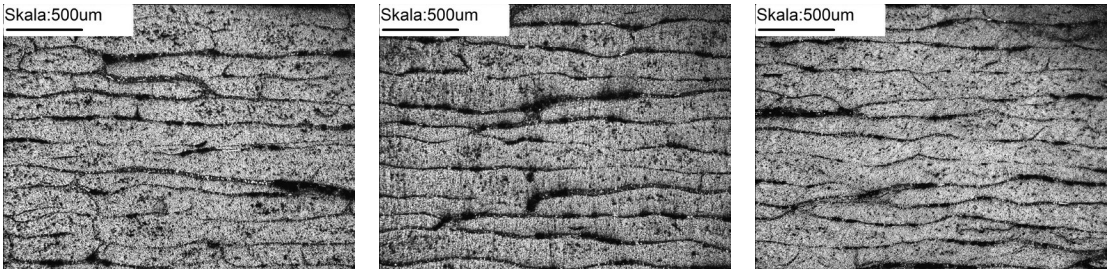

Fig.5. *Photographs of the carbon fiber composite microstructure at ×50 magnification for samples 1÷3*

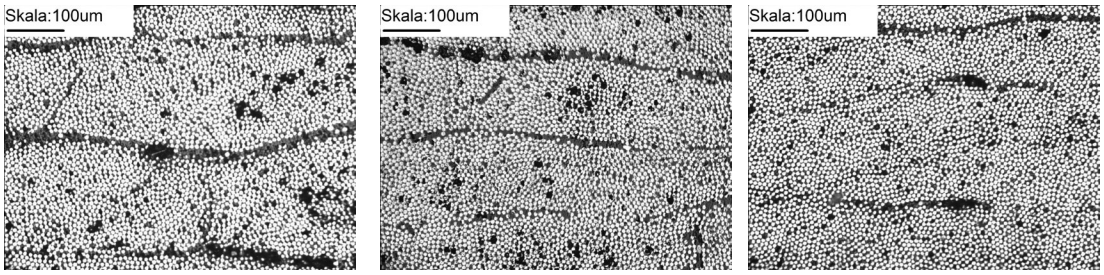

Fig.6. *Photographs of the carbon fiber composite microstructure at ×200 magnification for samples 1÷3*

Materials Research Proceedings 34 (2023) 43-52 https://doi.org/10.21741/9781644902691-6

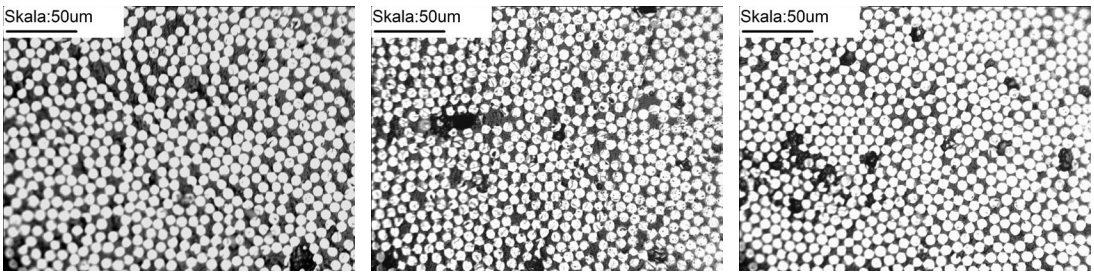

Fig.7. *Photographs of the carbon fiber composite microstructure at ×500 magnification for samples 1÷3*

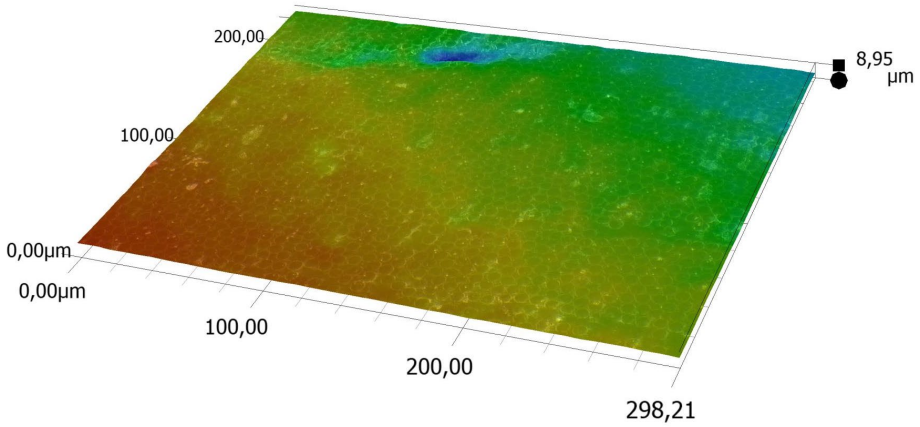

Fig. 8. *Topography of the epoxy/carbon fiber composite*

Table 4. *Tabulation of composite macrostructure surface measurement results.*

	EW composite	
	Volume fraction of fibers V_w [%]	**Volume fraction of voids Vp [%]**
Average for sample 1	70.3	10.0
Average for sample 2	64.4	8.5
Average for sample 3	65.3	6.0
Average for all the samples	66.7	8.2
Standard deviation	3.5	2.0
Volume fraction of resin ($100 – V_w – V_p$)	25.2	

Analysis of the microstructure of the epoxy/glass fiber-reinforced composite. Afterwards, tests were carried out for rings made of epoxy/glass fiber composite. In the first stage, the volume fraction of voids and discontinuities of the structure was analyzed at ×50 magnification (Fig. 9). After determining the void content, the content of the remaining components of the composite, i.e. fibers and resin, was studied at ×500 and ×1000 magnification (Fig. 10 and 11, Table 1). In addition, photographs of the topography of the sample surface were taken (example photograph - Fig. 12).

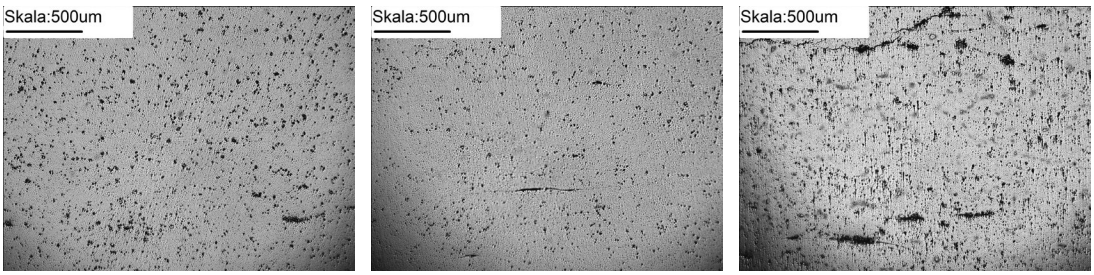

Fig. 9. *Photographs of the glass fiber composite microstructure at ×50 magnification for samples 1÷3*

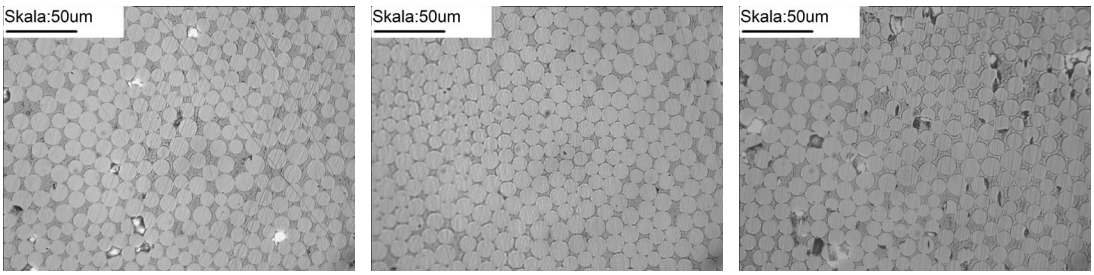

Fig. 10. *Photographs of the glass fiber composite microstructure at ×500 magnification for samples 1÷3*

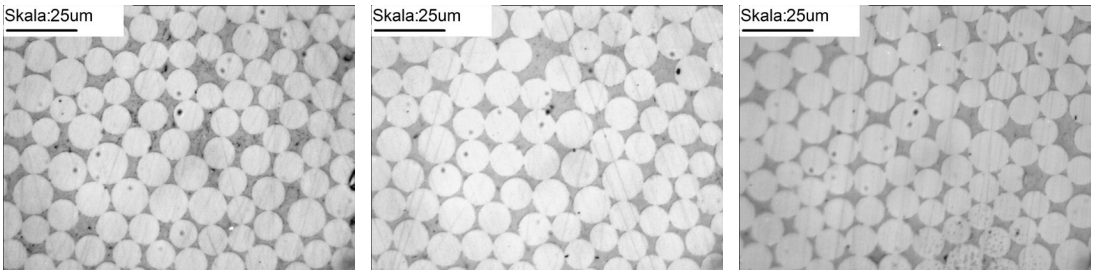

Fig. 11. *Photographs of the glass fiber composite microstructure at ×50 magnification for samples 1÷3*

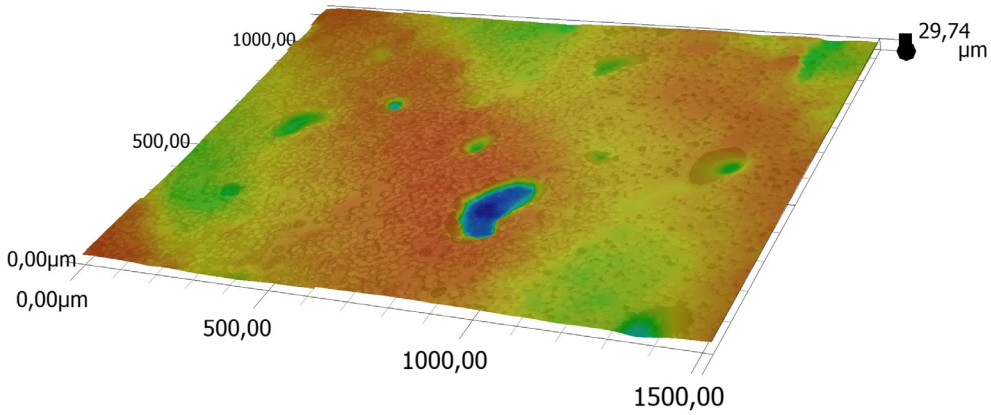

Fig. 12. *Topography of the epoxy/glass fiber-reinforced composite*

Table 5. *Tabulation of composite macrostructure surface measurement results.*

	EW composite	
	Volume fraction of fibers V_w [%]	**Volume fraction of fibers V_w [%]**
Average for sample 1	73.7	3.9
Average for sample 2	74.5	1.8
Average for sample 3	73.7	5.4
Average for all the samples	73.9	3.7
Standard deviation	2.1	2.5
Volume fraction of resin ($100 – V_w – V_p$)	22.4	

Conclusions

1. The structure of the distribution of roving bands in epoxy/carbon fiber composites (visible at ×50 and ×200 magnification) indicates that there is an undissolved protective layer on the outer surfaces of the roving bands, which is the reason for the lack of wettability, which in turn causes "discontinuity" of the composite. In the case of fiber composites, in which the preparation was used to cover the fibers, the structure is more homogeneous, apart from discontinuities in the form of voids;
2. Based on the statistical analysis (Tables 4 and 5), no significant and noticeable effect of fiber tension during winding on the density of "packing" fibers in composites, both epoxy/carbon fiber and epoxy/glass fiber reinforced, was found;
3. In the epoxy/carbon fiber composites, a greater "packing" was observed with increasing fiber tension, i.e. a smaller thickness of the discontinuity between the roving bands;
4. In both composites, the packing of fibers in the matrix is high; the values of 66.7% and 73.9% are considered almost borderline values (the highest tensile strength for glass fiber composites oscillates at about 72% of the fiber volume fraction in the composite [5]);
5. High content of fibers in the matrix may result in a lack of good wetting of the fibers with the resin, which may lead to reduced adhesion and delamination adhesion cracks, and as a result to "defibration" of the structure and utter destruction of the composite after the permissible load had been exceeded.

The conducted analysis focused on composites [12], although the essence of the issue falls within the scope of stereology [13-15]. The applied methods and analysis approaches can find broader application in similar cases of X-ray image observation [16], statistical analysis of material-related issues [17, 18], and process-related issues [19, 20]. Due to the projectional nature of the analyses, where 3D objects are projected onto a 2D space, nonparametric analyses [21-23] can be useful. The methodology should also be applicable in the analysis of complex surface layers such as DLC coatings [24].

References

[1] A. Błachut, P. Krysiak. Modelowanie w mikro- i makroskali nawijanej rury kompozytowej, Modelowanie Inżynierskie 35 (2018) 5-11.

[2] A. Błachut, P. Krysiak. Analysis of mechanical properties of epoxy resins used in composite high-pressure tank. Int. J. Eng. Sci. 4 (2016) 50-55.

[3] Composite Materials Handbook. Polymer matrix composites guidelines for characterization of structural materials, vol. 1, Department of Defense, Washington DC, 2002.

[4] H. Dąbrowski. Wytrzymałość polimerowych kompozytów włóknistych. Oficyna Wydawnicza Politechniki Wrocławskiej, Wrocław, 2002.

[5] W. Królikowski. Polimerowe kompozyty konstrukcyjne. PWN, Warszawa, 2012.

[6] P. Krysiak, A. Błachut, J. Kaleta. Theoretical and Experimental Analysis of Inter-Layer Stresses in Filament-Wound Cylindrical Composite Structures. Materials 14 (2021) art. 7037. https://doi.org/10.3390/ma14227037

[7] P. Krysiak, J. Kaleta, P. Gąsior, A. Błachut, R. Rybczyński. Identification of strains in a multilayer composite pipe. J. Sci. Mil. Acad. Land Forces 49 (2017) 272-282. https://doi.org/10.5604/01.3001.0010.7233

[8] P. Krysiak, R. Owczarek, W. Błażejewski, A. Błachut. Strength Testing and Ring Stiffness Testing of Underground Composite Pressure Pipes". Mater. Res. Proc. 17 (2020) 191-202. https://doi.org/10.21741/9781644901038-29

[9] Krosglass S.A. website. [online]. 2023. [viewed: 2023-01-31]. Available from: https://www.krosglass.pl

[10] Toho Tenax Europe website. [online]. 2023. [viewed: 2023-01-31]. Available from: https://www.chemeurope.com/

[11] Fatol Kunststoffen website. [online]. 2023. [viewed: 2023-01-31]. Available from: https://www.fatol.nl

[12] J. Korzekwa et al. Tribological behaviour of Al2O3/inorganic fullerene-like WS2 composite layer sliding against plastic, Int. J. Surf. Sci. Eng. 10 (2016) 570-584. https://doi.org/10.1504/IJSURFSE.2016.081035

[13] A. Gadek-Moszczak, P. Matusiewicz. Polish stereology – A historical review, Image Analysis and Stereology 36 (2017) 207-221. https://doi.org/10.5566/ias.1808

[14] J. Pietraszek, A. Szczotok, N. Radek. The fixed-effects analysis of the relation between SDAS and carbides for the airfoil blade traces. Arch. Metall. Mater. 62 (2017) 235-239. https://doi.org/10.1515/amm-2017-0035

[15] N. Radek et al. The impact of laser welding parameters on the mechanical properties of the weld, AIP Conf. Proc. 2017 (2018) art.20025. https://doi.org/10.1063/1.5056288

[16] B. Jasiewicz et al. Inter-observer and intra-observer reliability in the radiographic measurements of paediatric forefoot alignment, Foot Ankle Surg. 27 (2021) 371-376. https://doi.org/10.1016/j.fas.2020.04.015

[17] J. Pietraszek et al. The parametric RSM model with higher order terms for the meat tumbler machine process, Solid State Phenom. 235 (2015) 37-44. https://doi.org/10.4028/www.scientific.net/SSP.235.37

[18] J. Pietraszek et al. Challenges for the DOE methodology related to the introduction of Industry 4.0. Prod. Eng. Arch. 26 (2020) 190-194. https://doi.org/10.30657/pea.2020.26.33

[19] J. Pietraszek et al. Factorial approach to assessment of GPU computational efficiency in surrogate models, Adv. Mater. Res. 874 (2014) 157-162. https://doi.org/10.4028/www.scientific.net/AMR.874.157

[20] R. Dwornicka, J. Pietraszek. The outline of the expert system for the design of experiment, Prod. Eng. Arch. 20 (2018) 43-48. https://doi.org/10.30657/pea.2018.20.09

[21] J. Pietraszek. The modified sequential-binary approach for fuzzy operations on correlated assessments, LNAI 7894 (2013) 353-364. https://doi.org/10.1007/978-3-642-38658-9_32

[22] J. Pietraszek et al. Non-parametric assessment of the uncertainty in the analysis of the airfoil blade traces, METAL 2017 – 26th Int. Conf. Metall. Mater. (2017) 1412-1418. ISBN 978-8087294796

[23] J. Pietraszek et al. The non-parametric approach to the quantification of the uncertainty in the design of experiments modelling, UNCECOMP 2017 Proc. 2nd Int. Conf. Uncert. Quant. Comput. Sci. Eng. (2017) 598-604. https://doi.org/10.7712/120217.5395.17225

[24] N. Radek et al. Microstructure and tribological properties of DLC coatings, Mater. Res. Proc. 17 (2020) 171-176. https://doi.org/10.21741/9781644901038-26